

Alkylation–acylation of *p*-xylene with γ -butyrolactone or vinylacetic acid catalyzed by heteropolyacid supported on silica

Yuichi Kamiya^{a,b}, Yasunobu Ooka^b, Chisato Obara^b, Ryuichiro Ohnishi^c, Toshio Fujita^d,
Youhei Kurata^d, Katsuyuki Tsuji^d, Tetsuo Nakajyo^d, Toshio Okuhara^{a,b,*}

^a Faculty of Environmental Earth Science, Hokkaido University, N 10 W 5, Kita-ku, Sapporo 060-0810, Japan

^b Graduate School of Environmental Earth Science, Hokkaido University, N 10 W 5, Kita-ku, Sapporo 060-0810, Japan

^c Japan Science and Technology Agency, 4-1-8 Honcho, Kawaguchi 332-0012, Japan

^d Showa Denko K.K., 5-1 Ohgimachi, Kawasaki-ku, Kawasaki 210-0867, Japan

Available online 25 August 2006

Abstract

Friedel–Crafts-type reaction of *p*-xylene with γ -butyrolactone or vinylacetic acid over $\text{H}_4\text{SiW}_{12}\text{O}_{40}$ supported on SiO_2 have been investigated with different loadings of $\text{H}_4\text{SiW}_{12}\text{O}_{40}$. The catalytic performance of $\text{H}_4\text{SiW}_{12}\text{O}_{40}/\text{SiO}_2$ have been compared with those of typical solid acid catalysts such as zeolites, ion-exchanged resins, and binary oxides. $\text{H}_4\text{SiW}_{12}\text{O}_{40}$ supported on SiO_2 was superior in activity and selectivity to 5,8-dimethyl- α -tetralone compared to other catalysts for the reaction between *p*-xylene and γ -butyrolactone. SiO_2 -supported $\text{H}_4\text{SiW}_{12}\text{O}_{40}$ also was efficient for the formation of 3,4,7-tetramethyl- α -indanone from *p*-xylene and vinylacetic acid. The formation of 5,8-dimethyl- α -tetralone is extremely sensitive to the load of $\text{H}_4\text{SiW}_{12}\text{O}_{40}$ on SiO_2 , reaching a maximum at approximately 30 wt%, due to the change in the acid amount of the outermost surface as determined by benzonitrile-temperature programmed desorption. By analogy with reaction between 1,3,5-trimethylbenzene and γ -butyrolactone, the reaction pathway involves initial alkylation of *p*-xylene with γ -butyrolactone, followed by intramolecular acylation to 5,8-dimethyl- α -tetralone, which was supported by quantum calculations of γ -butyrolactone and protonated γ -butyrolactone.

© 2006 Elsevier B.V. All rights reserved.

Keywords: Heteropolyacid; Friedel–Crafts reaction; γ -Butyrolactone; Vinylacetic acid

1. Introduction

Friedel–Crafts alkylation and acylation of aromatic compounds are important reactions for the production of intermediates of fine chemicals [1]. However, traditional processes using liquid Lewis acid such as AlCl_3 , FeCl_3 , BF_3 , ZnCl_2 , and TiCl_4 , or Brønsted acids such as polyphosphoric acid and HF, can be environmentally harmful. Therefore, recent efforts have focused on developing environmentally friendly methods using solid acids for Friedel–Crafts reactions [2–18]. Zeolites are the most heavily studied catalysts for Friedel–Crafts reactions [1,19–26]. A commercial method for the acylation of anisol with acetic anhydride using a zeolite catalyst has been developed by Rhodia [19].

Heteropolyacids such as $\text{H}_3\text{PW}_{12}\text{O}_{40}$ and $\text{H}_4\text{SiW}_{12}\text{O}_{40}$ exhibit strong acidity and high activity for various acid-catalyzed reactions [27–31]. Since, as solid acids, heteropolyacids have low surface area ($\sim 6 \text{ m}^2 \text{ g}^{-1}$), supporting these heteropolyacids on oxidic carriers, especially SiO_2 , has been examined to enhance the density of acid sites available for reaction [27]. Reports have indicated that supported heteropolyacids show promise as catalysts for Friedel–Crafts reactions [28–36]. Kozhevnikov and coworkers reported that $\text{H}_3\text{PW}_{12}\text{O}_{40}/\text{SiO}_2$ possessed high activity for the reaction of anisole with acetic anhydride [32], and that pretreatment temperature of the catalyst significantly influenced the activity. Tagawa et al. demonstrated that the acidic cesium salt of $\text{H}_3\text{PW}_{12}\text{O}_{40}$ ($\text{Cs}_{2.5}\text{H}_{0.5}\text{PW}_{12}\text{O}_{40}$) was highly active for the reaction between benzene and benzoic anhydride [36].

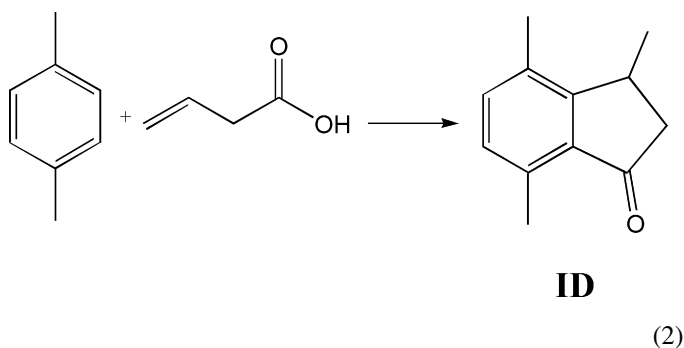
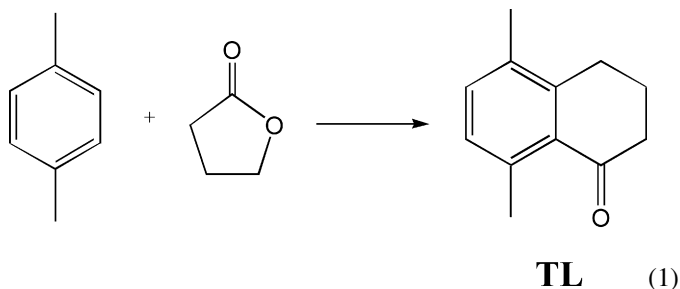
Derivatives of α -tetralone and α -indanone are important raw materials for medical applications. Practically, α -tetralone has been synthesized from benzene and succinic anhydride via multiple steps [37,38]. Friedel–Crafts reaction with γ -butyrolactone is intriguing because alkylation–acylation with

* Corresponding author at: Graduate School of Environmental Earth Science, Hokkaido University, N 10 W 5, Kita-ku, Sapporo 060-0810, Japan.

Tel.: +81 11 706 4513; fax: +81 11 706 4513.

E-mail address: oku@ees.hokudai.ac.jp (T. Okuhara).

an aromatic compound produces α -tetralone. Our preliminary report indicates that $\text{H}_4\text{SiW}_{12}\text{O}_{40}$ supported on SiO_2 catalyzed alkylation–acylation of *p*-xylene with γ -butyrolactone to 5,8-dimethyl- α -tetralone (Eq. (1)) [39,40] and this is an only report of the catalytic synthesis of this compound, while a system using an excess amount of AlCl_3 has been reported [41]. If vinylacetic acid is applicable for Friedel–Crafts reaction of *p*-xylene, 3,4,7-trimethyl- α -indanone is obtained (Eq. (2)) because vinylacetic acid also has the reactive vinyl and carboxylic functional groups



In the present study, the catalytic performance of $\text{H}_4\text{SiW}_{12}\text{O}_{40}/\text{SiO}_2$ was evaluated in the reaction of *p*-xylene with γ -butyrolactone to 5,8-dimethyl- α -tetralone (TL) or with vinylacetic acid to 3,4,7-trimethyl- α -indanone (ID); these were systematically compared with other typical solid acids including zeolites, binary oxides, and ion-exchange resins. The effects of $\text{H}_4\text{SiW}_{12}\text{O}_{40}$ loading amount on catalytic activity and selectivity for the formation of TL were investigated. Changes in activity and selectivity are discussed in conjunction with their acidic properties as assessed by temperature programmed desorption (TPD) using NH_3 and benzonitrile (BN) as probes. The reaction pathways for the formations of TL and ID also were examined by reactions using 1,3,5-trimethylbenzene instead of *p*-xylene, and quantum chemical calculations.

2. Experimental

2.1. Catalysts

$\text{H}_4\text{SiW}_{12}\text{O}_{40}$ and $\text{H}_3\text{PW}_{12}\text{O}_{40}$ were obtained from Nippon Inorganic Color and Chemical Co., and were calcined at 523 K in air before use. $\text{H}_4\text{SiW}_{12}\text{O}_{40}$ supported on SiO_2 ($\text{H}_4\text{SiW}_{12}\text{O}_{40}/\text{SiO}_2$) was prepared by a method reported previously [41]. The loadings of $\text{H}_4\text{SiW}_{12}\text{O}_{40}$ were adjusted to 10, 20, 30, 40, and 60 wt%. An aqueous solution (0.1 mol dm^{-3}) of $\text{H}_4\text{SiW}_{12}\text{O}_{40}$ in the amount necessary to achieve the intended

loading was added dropwise to SiO_2 (Aerosil 300, $274 \text{ m}^2 \text{ g}^{-1}$) at room temperature to form a wet solid. The wet solid was dried in an oven at 373 K overnight and then calcined at 523 K in air for 4 h. $\text{H}_4\text{SiW}_{12}\text{O}_{40}$ supported on mesoporous silica FSM-16 (supplied by Toyota Central R&D Labs., Inc.) was prepared in a manner similar to that for $\text{H}_4\text{SiW}_{12}\text{O}_{40}/\text{SiO}_2$. $\text{Cs}_{2.5}\text{H}_{0.5}\text{PW}_{12}\text{O}_{40}$ was prepared using aqueous solutions of $\text{H}_3\text{PW}_{12}\text{O}_{40}$ and Cs_2CO_3 as previously described [42]. This salt also was calcined at 523 K in air for 4 h.

$\text{WO}_3\text{--ZrO}_2$ ($\text{W}/\text{Zr}=0.1$) and $\text{MoO}_3\text{--ZrO}_2$ ($\text{Mo}/\text{Zr}=0.1$) were prepared by impregnating $\text{Zr}(\text{OH})_4$ (Daiichi Kigenso Co.) with aqueous solutions of $(\text{NH}_4)_{10}\text{W}_{12}\text{O}_{41}\cdot 5\text{H}_2\text{O}$ and $(\text{NH}_4)_6\text{Mo}_7\text{O}_{24}\cdot 4\text{H}_2\text{O}$, respectively, as reported previously [43], which were calcined at 1073 K in air for 3 h. Amberlyst-15 (Organo Co.) was used without pretreatment. Nafion-H (Wako Pure Chemical Ind. Ltd., NR50) and Nafion- SiO_2 composite (Dupont, SAC-13, Nafion 13 wt%) were dried overnight at 373 K just before use. Zeolites such as H- β (Süd-Chemie, $\text{Si}/\text{Al}=12.5$), H-ZSM-5 (Tosoh, HSZ-860HOA, $\text{Si}/\text{Al}=37$), H-Y (Reference Catalyst of the Catalysis Society of Japan, JRC-H-4.8, $\text{Si}/\text{Al}=4.8$), H-mordenite (Reference Catalyst of the Catalysis Society of Japan, JRC-Z-HM(10), $\text{Si}/\text{Al}=10$) were pretreated at 723 K in air for 4 h. $\text{SiO}_2\text{--Al}_2\text{O}_3$ (Reference Catalyst of the Catalysis Society of Japan, JRC-SAL-2) also was used after calcination at 673 K in air for 2 h.

2.2. Characterization

NH_3 -TPD was characterized using a Multitask TPD system (BEL Japan, Inc.) equipped with a mass spectrometer. After the sample (200 mg) was pretreated in a flow of He at 523 K for 1 h, it was exposed to NH_3 (100 Torr) for 0.5 h at 373 K. The chamber was subsequently purged with a He flow at 373 K for 0.5 h to remove physisorbed NH_3 . The temperature of the sample was raised at a rate of 10 K min^{-1} to 973 K, and the desorption rate of NH_3 was monitored using $m/e=16$.

The benzonitrile-TPD (BN-TPD) profile was obtained using a custom made TPD system equipped with an FID detector. After the sample was pretreated under N_2 flow at 523 K for 2 h, it was exposed at 373 K for 1 h to a N_2 flow bubbled through a saturator of BN at room temperature. The excess BN was removed under N_2 flow at 373 K for 1 h and then 393 K for 1 h. The temperature of the sample then was raised at a rate of 10 K min^{-1} to 973 K under N_2 flow while the desorption rate of BN was monitored by the FID detector.

2.3. Quantum chemical calculation

Geometric structure optimization and charge distributions for γ -butyrolactone and protonated γ -butyrolactone were determined by *ab initio* quantum calculation using the Gaussian 98 program. B3YLP/6-31+ G^* was adapted as a base set.

2.4. Catalytic reaction of *p*-xylene with γ -butyrolactone or vinylacetic acid

Reaction of *p*-xylene with γ -butyrolactone (GBL) was conducted in a stainless autoclave (Taiatsu Techno Co., Model

Table 1
Catalytic data for synthesis of 5,8-dimethyl- α -tetralone from *p*-xylene and γ -butyrolactone over various solid acids

Catalyst	Conversion (%)	Yield (%)					Selectivity to TL ^{a,b} (%)
		TL ^a	4-BA ^a	ID ^a	UN ^a	OT ^a	
20 wt% H ₄ SiW ₁₂ O ₄₀ /SiO ₂	74	54	1	3	8	8	73
60 wt% H ₄ SiW ₁₂ O ₄₀ /FSM-16	94	62	2	6	13	11	66
H ₄ SiW ₁₂ O ₄₀	47	7	0	1	3	36	15
H ₃ PW ₁₂ O ₄₀	51	9	0	1	1	40	18
Cs _{2.5} H _{0.5} PW ₁₂ O ₄₀	33	20	0	3	5	5	61
SiO ₂ -Al ₂ O ₃	25	2	0	0	8	15	8
WO ₃ -ZrO ₂	28	21	0	1	6	0	75
MoO ₃ -ZrO ₂	4	2	0	0	2	0	50
H- β	49	11	10	0	3	25	22
H-ZSM-5	33	5	3	0	6	19	15
H-Y	44	11	1	0	1	31	25
Amberlyst 15	55	23	1	6	7	18	42
Nafion-H	27	14	0	1	5	7	52
Nafion-SiO ₂	25	15	0	1	9	0	60

Reaction conditions: catalyst weight 0.16 g, *p*-xylene 81 mmol, γ -butyrolactone 0.74 mmol, reaction temperature 483 K, and reaction time 2 h.

^a TL = 5,8-dimethyl- α -tetralone, 4-BA = 4-(2,5-dimethylphenyl) butyric acid, ID = 3,4,7-trimethyl- α -indanone, UN = unidentified products which were detected by GC of the reaction mixture, and OT = products not detected by GC of the reaction mixture.

^b Selectivity is defined as the percentage of TL among all the products.

TPR-5, 100 cm³). A mixture of *p*-xylene (Wako Pure Chemical Ind. Ltd., 81 mmol) and GBL (Wako Pure Chemical Ind. Ltd., 0.74 mmol), and 0.16 g of catalyst were introduced into the reactor. After the inside of the reactor was purged with N₂, the temperature was increased to 483 K with vigorous stirring. After reaction at 483 K for 2 h, the reactor was cooled rapidly to room temperature, and the solid catalyst separated from the suspension by filtration. Elemental analysis of the recovered spent catalyst for carbon was carried out at the Center for Instrumental Analysis, Hokkaido University, after the filtered catalyst was dried at 373 K overnight. The resulting filtrate was analyzed by FID-GC (Shimadzu, GC-14B) equipped with a capillary column of ZB-WAX (30 m \times 0.25 mm, Zebron). Cyclohexanol was used as the internal standard for GC analysis. The conversion, yield, and selectivity toward TL were defined as:

$$\text{conversion (\%)} = 100 \times \frac{\text{mol of GBL in filtrate}}{\text{mol of GBL added}},$$

$$\text{yield (\%)} = 100 \times \frac{\text{mol of product}}{\text{mol of GBL added}},$$

$$\text{selectivity to TL (\%)} = 100 \times \frac{\text{yield of TL}}{\text{conversion of GBL}}$$

The reaction of *p*-xylene with vinylacetic acid was conducted in a manner similar to that of *p*-xylene with GBL except for the use of vinylacetic acid (Wako Pure Chemical Ind. Ltd., 0.76 mmol), a catalyst weight of 0.2 g, and reaction temperature of 433 K.

Products were identified using GC-MS (GC: Shimadzu GC-17A with 30 m \times 0.25 mm capillary column of ZB-WAX, MS: Shimadzu GCQP-5050).

3. Results and discussion

3.1. Catalytic performance of various solid acids

Catalytic results for the reaction of *p*-xylene with GBL over various solid acids are summarized in Table 1. The main product was 5,8-dimethyl- α -tetralone (TL) and formation of 4-(2,5-dimethylphenyl) butyric acid (4-BA) and 3,4,7-trimethyl- α -indanone (ID) was negligibly small over typical solid acids under the reaction conditions, while an amount of 4-BA was formed only over H- β (yield of 4-BA, 10%). The gas chromatograms showed the formation of a small amount of several other unidentified products, designated as UN in Table 1. Considering the material balance of GBL, there were products adhering tenaciously to the catalyst and these were classified as OT in Table 1. For H₄SiW₁₂O₄₀ supported on SiO₂, yields of OT were 14, 8, 26, 25, 25, and 34% for 10, 20, 30, 40, 60, and 100 wt% loadings, respectively (Fig. 1). Carbon content of the spent H₄SiW₁₂O₄₀/SiO₂ catalysts, which were dried at 373 K overnight prior to the elemental analysis, were 1.8, 2.6, 4.5, 5.8, 6.7, and 6.1 wt%, which correspond to 10, 12, 22, 28, 33, and 29% of the initial amount of GBL, for 10, 20, 30, 40, 60, and 100 wt% H₄SiW₁₂O₄₀/SiO₂, respectively. Since yields of OT basically agreed with values calculated from the carbon content of the spent catalysts, most OT compounds probably are oligomers of GBL or GBL strongly adsorbed on the catalyst.

The zeolites used in this study were not effective catalysts for the formation of TL. While H- β , H-ZSM-5, and H-Y showed moderate conversions, selectivity toward TL was very low, probably due to the relatively larger size of TL compared to the pore sizes of these zeolites, causing the formation of products such as oligomers of GBL. Reaction using WO₃-ZrO₂ selectively yielded TL, but with low activity.

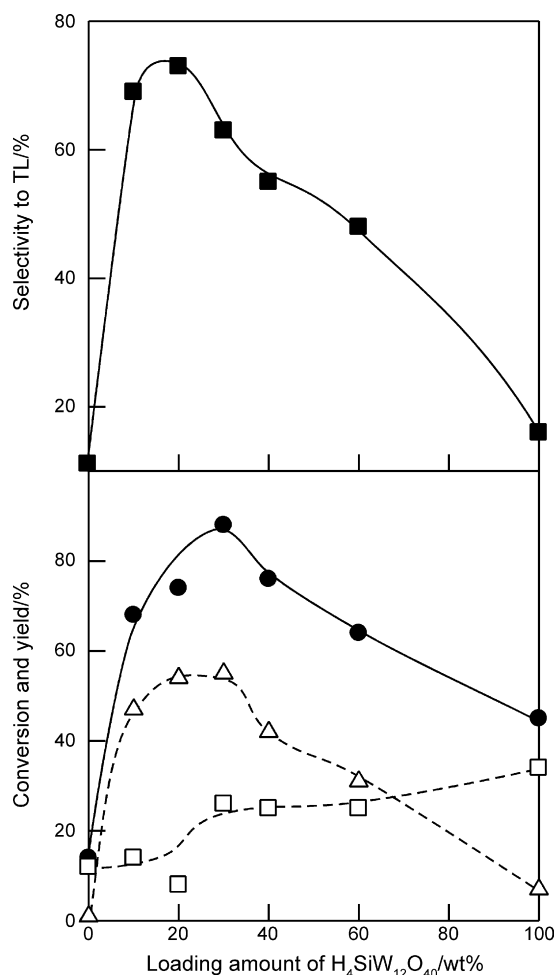


Fig. 1. Effects of loading amount of $\text{H}_4\text{SiW}_{12}\text{O}_{40}$ on SiO_2 for synthesis of 5,8-dimethyl- α -tetralone (TL) from *p*-xylene and γ -butyrolactone (GBL). Reaction conditions: catalyst weight 0.16 g, *p*-xylene 81 mmol, GBL 0.74 mmol, reaction temperature 483 K, and reaction time 2 h. (●) Conversion of GBL, yield of (Δ) TL and (□) OT, and (■) selectivity toward TL.

Ion-exchanged resins such as Amberlyst 15, Nafion-H, and Nafion- SiO_2 composite showed activity for the formation of TL. Nafion- SiO_2 showed relatively high selectivity toward TL (60%), but was less active.

Data in Table 1 demonstrate that $\text{H}_4\text{SiW}_{12}\text{O}_{40}$ supported on SiO_2 and mesoporous silica FSM-16 exhibited both high activity and selectivity toward TL; the highest selectivity toward TL (73%) was obtained over 20 wt% $\text{H}_4\text{SiW}_{12}\text{O}_{40}/\text{SiO}_2$ and the highest yield of TL was obtained for 60 wt% $\text{H}_4\text{SiW}_{12}\text{O}_{40}/\text{FSM-16}$, whereas the formation of OT was small over these catalysts, resulting in high selectivity toward TL. Unsupported heteropolyacids, such as $\text{H}_4\text{SiW}_{12}\text{O}_{40}$ and $\text{H}_3\text{PW}_{12}\text{O}_{40}$, were active for converting GBL, but mainly yielded OT. These results demonstrate that $\text{H}_4\text{SiW}_{12}\text{O}_{40}$ supported on SiO_2 and FSM-16 were effective catalysts for the one-step synthesis of TL from *p*-xylene and GBL.

Table 2 presents results of the reaction between *p*-xylene and vinylacetic acid to 3,4,7-trimethyl- α -indanone (ID) over various solid acids. Typical solid acids, except for SiO_2 -supported $\text{H}_4\text{SiW}_{12}\text{O}_{40}$, Nafion-H, and Nafion- SiO_2 , were

essentially inactive for the formation of ID. In contrast, 20 wt% $\text{H}_4\text{SiW}_{12}\text{O}_{40}/\text{SiO}_2$ gave ID at 19% yield under the reaction conditions, while only a small amount of ID was formed over Nafion-H and Nafion- SiO_2 composite. The strong acidic nature of the heteropolyacids as well as Nafion-H may be required for the formation of ID. Optimization of $\text{H}_4\text{SiW}_{12}\text{O}_{40}$ loading (40 wt%), reaction time (4 h), and reaction temperature (463 K) produced a maximum yield of ID (44%), as shown in Table 2.

3.2. Effect of loading amount of $\text{H}_4\text{SiW}_{12}\text{O}_{40}$ on activity and selectivity for reaction of *p*-xylene with γ -butyrolactone, and acidic properties of SiO_2 -supported $\text{H}_4\text{SiW}_{12}\text{O}_{40}$

Fig. 1 shows the effect of loading amount of $\text{H}_4\text{SiW}_{12}\text{O}_{40}$ on conversion of GBL, yields of TL and OT, and selectivity to TL for the reaction of *p*-xylene with GBL, with SiO_2 as a support. The conversion and yield of TL increased with loading amount. Note that the yield of TL reached a maximum of 55% at 30 wt%; a further increase in the loading amount caused a decrease in yield. In contrast, the yield of OT increased monotonically with loading amount of $\text{H}_4\text{SiW}_{12}\text{O}_{40}$. As a consequence, the selectivity toward TL showed a maximum (73%) at 20 wt% loading. At higher loading levels, the selectivity drastically decreased with loading amount.

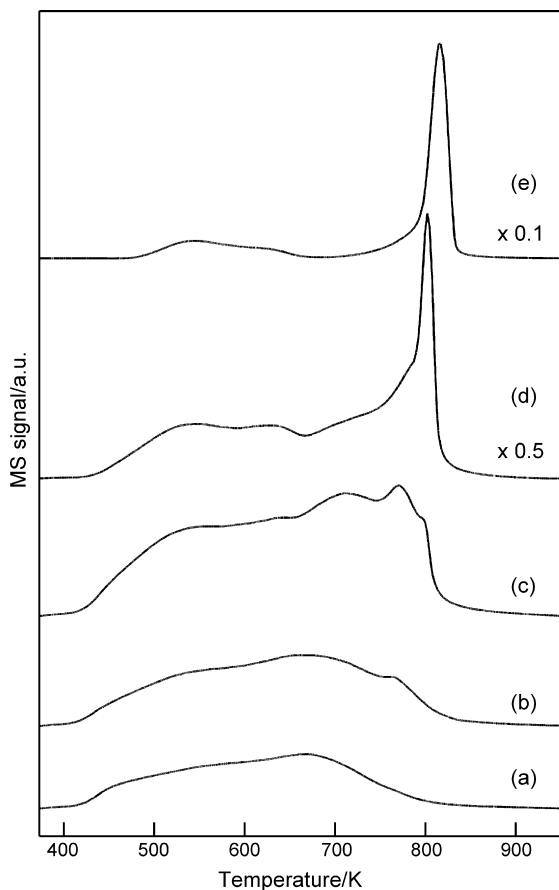
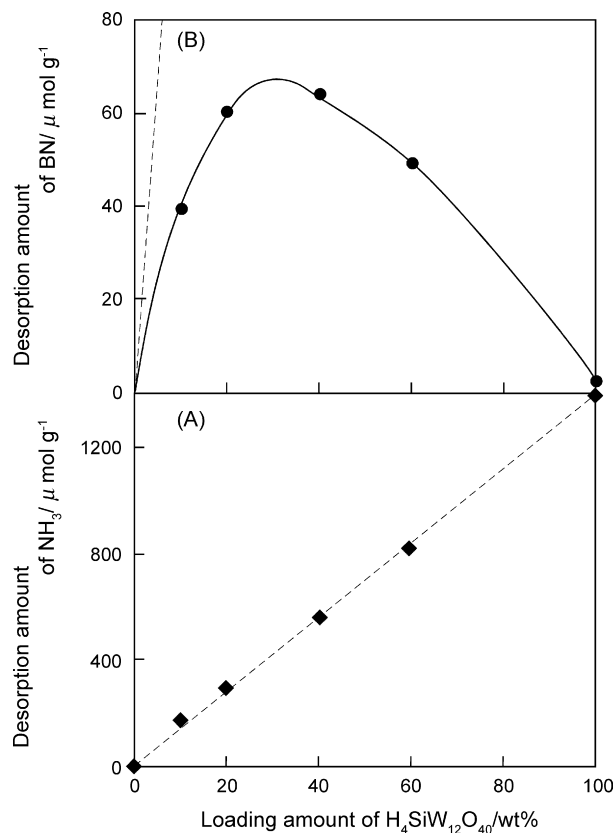
Fig. 2 shows NH_3 -TPD profiles of $\text{H}_4\text{SiW}_{12}\text{O}_{40}/\text{SiO}_2$ with different $\text{H}_4\text{SiW}_{12}\text{O}_{40}$ loadings. The amount of desorption of NH_3 from $\text{H}_4\text{SiW}_{12}\text{O}_{40}/\text{SiO}_2$ is plotted as a function of $\text{H}_4\text{SiW}_{12}\text{O}_{40}$ loading in Fig. 3A, in which the broken line represents the total amount of protons present in $\text{H}_4\text{SiW}_{12}\text{O}_{40}/\text{SiO}_2$ calculated from the loading of $\text{H}_4\text{SiW}_{12}\text{O}_{40}$. It is known that NH_3 can interact with acid sites of the bulk heteropolyacid [27]. As shown in Fig. 3A, the desorption amount of NH_3 from $\text{H}_4\text{SiW}_{12}\text{O}_{40}/\text{SiO}_2$ agreed well with the calculated amount of protons present in the bulk of $\text{H}_4\text{SiW}_{12}\text{O}_{40}/\text{SiO}_2$. This correlation clearly indicates that the NH_3 -TPD profile indicated acidity in the bulk of $\text{H}_4\text{SiW}_{12}\text{O}_{40}/\text{SiO}_2$. A sharp peak at about 800 K was observed from NH_3 -TPD of $\text{H}_4\text{SiW}_{12}\text{O}_{40}$ (Fig. 2e). In contrast, the profiles of $\text{H}_4\text{SiW}_{12}\text{O}_{40}/\text{SiO}_2$ consisted of a few broad peaks with the maximum desorption rate shifted toward lower temperatures upon decrease of $\text{H}_4\text{SiW}_{12}\text{O}_{40}$ loading. Notably, 10 and 20 wt% $\text{H}_4\text{SiW}_{12}\text{O}_{40}/\text{SiO}_2$ did not produce the NH_3 desorption peak near 800 K, which was clearly observed for the parent $\text{H}_4\text{SiW}_{12}\text{O}_{40}$ and $\text{H}_4\text{SiW}_{12}\text{O}_{40}/\text{SiO}_2$ with high loadings (>40 wt%). These results indicate that the supporting $\text{H}_4\text{SiW}_{12}\text{O}_{40}$ on SiO_2 weakens the acid strength in the bulk of $\text{H}_4\text{SiW}_{12}\text{O}_{40}$. Based on microcalorimetry measurements of the heat of absorption of NH_3 , Kozhevnikov and coworkers reported that the acid strength of $\text{H}_3\text{PW}_{12}\text{O}_{40}$ decreased significantly when supported on SiO_2 [44]. Other reports indicate that protons of $\text{H}_3\text{PW}_{12}\text{O}_{40}$ react with OH groups on SiO_2 to form $-\text{OH}_2^+(\text{H}_2\text{PW}_{12}\text{O}_{40}^-)$ [45,46]. Similar interaction between $\text{H}_4\text{SiW}_{12}\text{O}_{40}$ and $-\text{OH}$ on SiO_2 would reduce acid strength in the bulk of $\text{H}_4\text{SiW}_{12}\text{O}_{40}$ for $\text{H}_4\text{SiW}_{12}\text{O}_4/\text{SiO}_2$.

Our previous report demonstrates that BN was not adsorbed into the bulk $\text{H}_4\text{SiW}_{12}\text{O}_{40}$ due to large molecule size and low basicity; instead, it was adsorbed only onto the outermost surface of $\text{H}_4\text{SiW}_{12}\text{O}_{40}$ crystallites at 393 K [47]. In addition,

Table 2

Catalytic data for synthesis of 3,4,7-tetramethyl- α -indanone from *p*-xylene and vinylacetic acid over various solid acids

Catalyst	Conversion (%)	Yield (%)					Selectivity to ID ^b (%)
		ID ^a	3-BA ^a	CA ^a	UN ^a	OT ^a	
20 wt% H ₄ SiW ₁₂ O ₄₀ /SiO ₂	94	19	3	52	2	18	20
40 wt% H ₄ SiW ₁₂ O ₄₀ /SiO ₂ ^c	99	44	17	8	16	14	44
H ₄ SiW ₁₂ O ₄₀	89	5	9	70	3	2	6
H ₃ PW ₁₂ O ₄₀	79	1	14	53	2	9	1
Cs _{2.5} H _{0.5} PW ₁₂ O ₄₀	89	1	20	56	12	0	1
SiO ₂ -Al ₂ O ₃	45	0	0	8	37	0	0
WO ₃ -ZrO ₂	37	1	16	13	7	0	3
MoO ₃ -ZrO ₂	50	1	20	11	18	0	2
H- β	91	1	37	28	14	11	1
H-ZSM-5	91	0	0	74	11	6	0
H-Y	67	0	3	16	21	27	0
H-mordenite	46	0	0	4	3	39	0
Amberlyst 15	99	1	0	4	94	0	1
Nafion-H	82	12	3	24	20	23	15
Nafion-SiO ₂	95	8	13	69	3	3	8

Reaction conditions: catalyst weight 0.2 g, *p*-xylene 81 mmol, vinylacetic acid 0.76 mmol, reaction temperature 433 K, and reaction time 2 h.^a ID = 3,4,7-tetramethyl- α -indanone, 3-BA = 3-(2,5-dimethylphenyl) butyric acid, CA = crotonic acid, UN = unidentified products which were detected by GC of the reaction mixture, and OT = products not detected by GC of the reaction mixture.^b Selectivity is defined as the percentage of ID among all the products.^c Reaction was carried out at 463 K for 4 h.Fig. 2. NH₃-TPD profile of H₄SiW₁₂O₄₀/SiO₂. (a) 10 wt% H₄SiW₁₂O₄₀/SiO₂, (b) 20 wt% H₄SiW₁₂O₄₀/SiO₂, (c) 40 wt% H₄SiW₁₂O₄₀/SiO₂, (d) 60 wt% H₄SiW₁₂O₄₀/SiO₂ and (e) H₄SiW₁₂O₄₀.Fig. 3. Desorption amounts of NH₃ and benzonitrile from H₄SiW₁₂O₄₀/SiO₂. (A) NH₃ and (B) benzonitrile (BN). Broken lines represent the total amount of protons calculated from the loading amount of H₄SiW₁₂O₄₀.

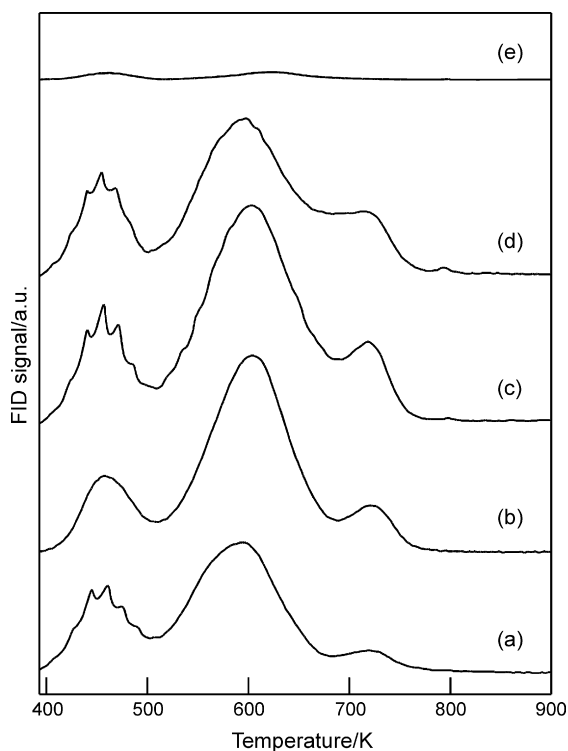


Fig. 4. Benzonitrile-TPD profile of $\text{H}_4\text{SiW}_{12}\text{O}_{40}/\text{SiO}_2$. (a) 10 wt% $\text{H}_4\text{SiW}_{12}\text{O}_{40}/\text{SiO}_2$, (b) 20 wt% $\text{H}_4\text{SiW}_{12}\text{O}_{40}/\text{SiO}_2$, (c) 40 wt% $\text{H}_4\text{SiW}_{12}\text{O}_{40}/\text{SiO}_2$, (d) 60 wt% $\text{H}_4\text{SiW}_{12}\text{O}_{40}/\text{SiO}_2$, and (e) $\text{H}_4\text{SiW}_{12}\text{O}_{40}$.

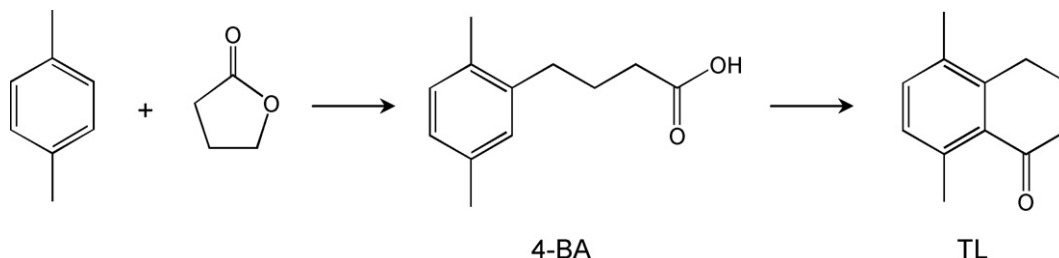
BN was not adsorbed on SiO_2 at this temperature. Thus, the acidic properties of the outermost surface of $\text{H}_4\text{SiW}_{12}\text{O}_{40}/\text{SiO}_2$ can be assessed with BN-TPD. Fig. 4 shows BN-TPD profiles of $\text{H}_4\text{SiW}_{12}\text{O}_{40}/\text{SiO}_2$. The desorption amounts of BN are shown in Fig. 3B as a function of $\text{H}_4\text{SiW}_{12}\text{O}_{40}$ loading; the broken line represents the total amount of protons calculated from the loading of $\text{H}_4\text{SiW}_{12}\text{O}_{40}$. In contrast to the desorption amounts of NH_3 shown in Fig. 3A, the amount of desorption of BN was below the calculated total amount of protons in $\text{H}_4\text{SiW}_{12}\text{O}_{40}/\text{SiO}_2$ (broken line in Fig. 3) and attained a maximum at 40 wt% loading. Reactions catalyzed by heteropolyacids can be divided into surface reactions and bulk reactions [1], with non-polar molecules such as hydrocarbons driving surface reactions and polar molecules such as alcohol driving bulk reactions. The trend shown in Fig. 3B was similar to that for the yield of TL as shown in Fig. 1. Thus, it is likely that the high activity found for 20–30 wt% $\text{H}_4\text{SiW}_{12}\text{O}_{40}/\text{SiO}_2$ accounts for the large amount of acid sites on the outermost surface. As shown

in Fig. 4, temperature of the maximum desorption rate of BN, which corresponds to the acid strength of the outermost surface, was barely influenced by $\text{H}_4\text{SiW}_{12}\text{O}_{40}$ loading. On the other hand, reports on skeletal isomerizations of *n*-pentane and *n*-heptane over $\text{Pd-H}_4\text{SiW}_{12}\text{O}_{40}/\text{SiO}_2$, which are classified into the surface reaction, suggested that the acid strength of the outermost surface of $\text{H}_4\text{SiW}_{12}\text{O}_{40}/\text{SiO}_2$ weakened with decrease of the loading amount [47,48]. Thus, to assess the acid strength of the outermost surface of $\text{H}_4\text{SiW}_{12}\text{O}_{40}/\text{SiO}_2$, further investigations on BN-TPD such as analysis of desorbed molecules using mass spectrometer would be required.

The dependency of the yield of OT, which was mainly oligomer of GBL, cannot be explained by acid amount and strength of the outermost surface. Thus, it is reasonable to consider that the formation of OT occurs in the bulk of $\text{H}_4\text{SiW}_{12}\text{O}_{40}$. Assuming that two BN adsorb on a heteropolyacid located on the outermost surface of $\text{H}_4\text{SiW}_{12}\text{O}_{40}/\text{SiO}_2$, the average number of layers of $\text{H}_4\text{SiW}_{12}\text{O}_{40}$ units on the SiO_2 surface was 1.8, 4.6, 8.7, and 16.9 for 10, 20, 40, and 60 wt% $\text{H}_4\text{SiW}_{12}\text{O}_{40}/\text{SiO}_2$, respectively. In addition, as shown in Fig. 2, the acid strength in the bulk of $\text{H}_4\text{SiW}_{12}\text{O}_{40}$ gradually decreased with $\text{H}_4\text{SiW}_{12}\text{O}_{40}$ loading. Both the paucity of the bulk $\text{H}_4\text{SiW}_{12}\text{O}_{40}$ and weakness of the acid strength in the bulk of $\text{H}_4\text{SiW}_{12}\text{O}_{40}$ help explain the low selectivity for formation of OT over $\text{H}_4\text{SiW}_{12}\text{O}_{40}/\text{SiO}_2$ with low loadings, causing high selectivity toward TL.

3.3. Reaction pathway for formation of 5,8-dimethyl- α -tetralone and 3,4,7-trimethyl- α -indanone over $\text{H}_4\text{SiW}_{12}\text{O}_{40}/\text{SiO}_2$

The mechanism of the Friedel–Crafts reaction of *p*-xylene with GBL is debatable because two possible reaction pathways can form TL: one involves initial alkylation of *p*-xylene with GBL to form 4-(2,5-dimethylphenyl) butyric acid (4-BA) as an intermediate followed by intramolecular acylation to TL; the other involves initial acylation with the formation of 4-hydroxy-1-(2,5-dimethylphenyl)-butan-1-one as an intermediate followed by intramolecular alkylation. To identify the correct mechanism, substituting 1,3,5-trimethylbenzene for *p*-xylene is informative because intermolecular reaction between 1,3,5-trimethylbenzene and GBL can occur, but subsequent intramolecular alkylation or acylation is prevented by the steric hindrance caused by two methyl groups located adjacent to the position of GBL reaction. A previous report demonstrated that the reaction of 1,3,5-trimethylbenzene with GBL at 453 K over solid acids, including $\text{H}_3\text{PW}_{12}\text{O}_{40}$ and $\text{H}_4\text{SiW}_{12}\text{O}_{40}$ alone and



Scheme 1.

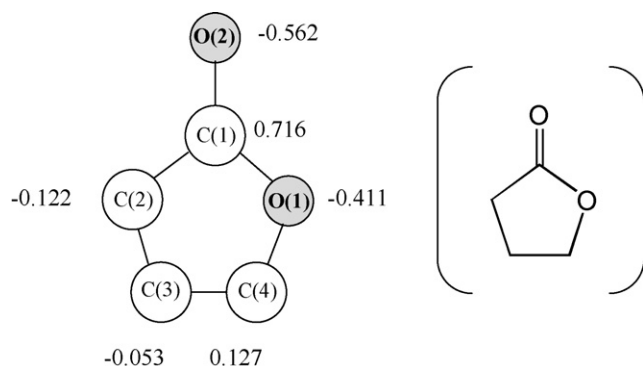


Fig. 5. Electronic charges of each atom for γ -butyrolactone estimated by quantum chemical calculation.

supported on SiO_2 , gave only an alkylation product [41]. By analogy, reaction between *p*-xylene and GBL occurs first by alkylation of *p*-xylene with GBL to form 4-BA, followed by transformation into TL by intramolecular acylation, as shown in Scheme 1. In fact, 4-hydroxy-1-(2,5-dimethylphenyl)-butan-1-one, which is a possible intermediate in the acylation–alkylation sequence, was not detected by GC or GC–MS analysis of the reaction mixture.

Fig. 5 shows electronic charges of each atom for GBL as estimated by the quantum chemical calculations, for which the structure of GBL was optimized. While GBL possesses two negatively charged oxygen atoms, an ester [O(1)] and carbonyl oxygen [O(2)], as shown in Fig. 5, the negative charge of O(2) was greater than that of O(1), suggesting that the basicity of the carbonyl oxygen is greater than that of the ester oxygen. If a proton attacks a carbonyl oxygen in GBL, alkylation occurs. In contrast, if a proton attacks an ester oxygen, acylation occurs. According to the reaction pathway we proposed (Scheme 1), over $\text{H}_4\text{SiW}_{12}\text{O}_{40}/\text{SiO}_2$ under the reaction conditions the proton would attack the carbonyl oxygen of GBL, taking place the alkylation. The negative charges of oxygens in GBL estimated

by the quantum chemical calculation is consistent with the reaction pathway.

The bond lengths of GBL and protonated GBL, in which a carbonyl oxygen is protonated, are shown in Fig. 6. The structures of these molecules were optimized using quantum chemical calculations. When the GBL carbonyl oxygen [O(2)] was protonated, the O(1)–C(4) bond increased in length from 0.1447 to 0.1500 nm, while the O(1)–C(1) and C(1)–C(2) bonds became shorter. This suggests that the dissociation of the O(1)–C(4) bond is induced by protonation of the carbonyl oxygen in GBL. Thus, we propose that GBL is activated by proton attack, followed by nucleophilic addition of *p*-xylene to the positively charged carbon atom of GBL to form 4-BA and intramolecular acylation by a second proton attack to TL, as shown in Scheme 2. As summarized in Table 1, yields of 4-BA over solid acids, except for H- β were very low under the reaction conditions, allowing rapid intramolecular acylation of 4-BA.

For reaction between *p*-xylene and vinylacetic acid, two possible sequences, acylation–alkylation or alkylation–acylation, also are possible. Reaction between 1,3,5-trimethylbenzene and vinylacetic acid over 10 wt% $\text{H}_4\text{SiW}_{12}\text{O}_{40}/\text{SiO}_2$ was conducted under the same reaction conditions as those for *p*-xylene. GC analysis indicated that the yields of 3-(2,4,6-trimethylphenyl)butyric acid, crotonic acid, and unidentified products were 29, 35, and 28%, respectively, at 96% conversion, while the products formed by acylation such as (2,4,6-trimethylphenyl)-3-butene-1-one and (2,4,6-trimethylphenyl)-2-butene-1-one were not detected by GC analysis. Thus, under these reaction conditions, alkylation of 1,3,5-trimethylbenzene with vinylacetic acid proceeded exclusively, whereas acylation did not occur over 10 wt% $\text{H}_4\text{SiW}_{12}\text{O}_{40}/\text{SiO}_2$. In a separate experiment, the formation rate of ID from *p*-xylene and crotonic acid was more than 10-fold slower than that from reaction between *p*-xylene and vinylacetic acid at 433 K over 10 wt% $\text{H}_4\text{SiW}_{12}\text{O}_{40}/\text{SiO}_2$, indicating that the contribution of crotonic acid to the formation of ID was small. The proposed reaction pathway is as follows.

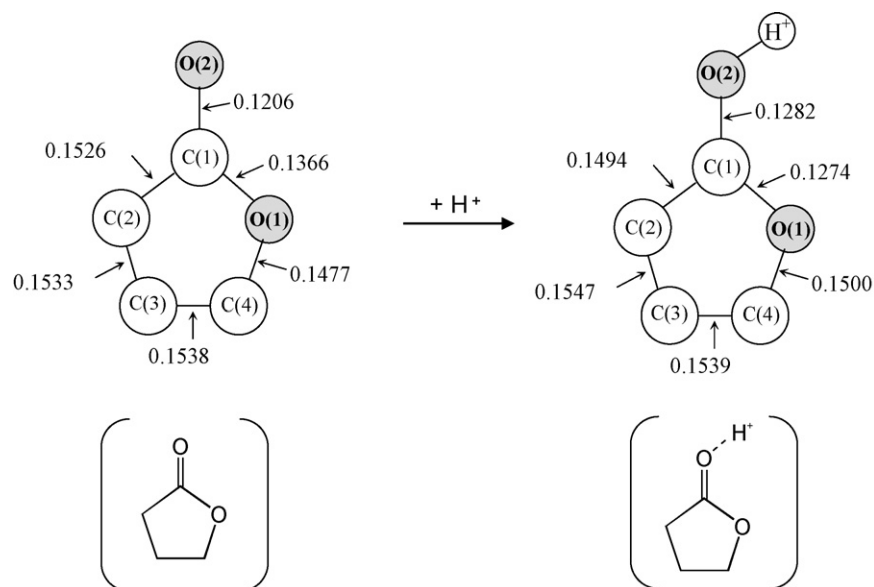
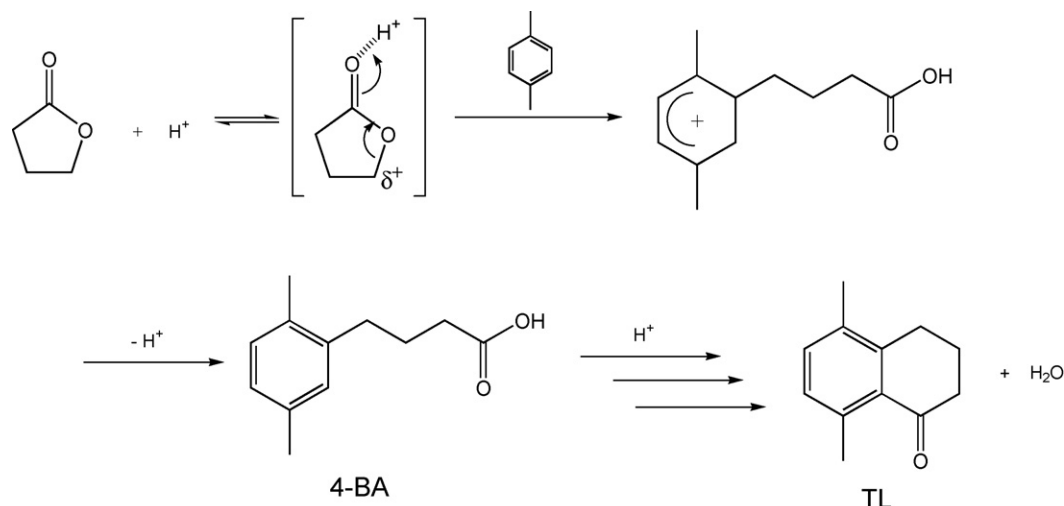
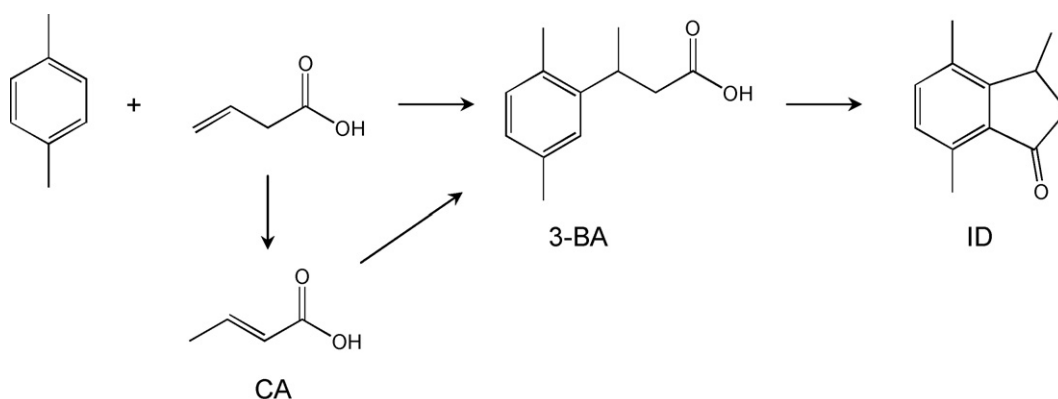


Fig. 6. Bond length for γ -butyrolactone and protonated γ -butyrolactone estimated by quantum chemical calculation.



Scheme 2.



Scheme 3.

First alkylation of *p*-xylene with vinylacetic acid occurs to form 3-BA, followed by intramolecular acylation to ID, as shown in Scheme 3. Acylation of *p*-xylene with vinylacetic acid does not proceed, but the intramolecular acylation of 3-BA does, probably due to the activation of the benzene ring by addition of vinylacetic acid or effective intramolecular acylation.

Acknowledgements

This work was partly supported by Core Research for Evolutional Science and Technology (CREST) of the Japan Science and Technology Corporation (JST). This work also was supported by the New Energy and Industrial Technology Development Organization (NEDO) and by the Japan Chemical Industry Association (JCII).

References

- [1] G.A. Olah, Friedel–Crafts and Related Reactions, vols. I–IV, Wiley/Interscience, New York, 1963–1964.
- [2] M. Casagrande, L. Storaro, M. Lenarda, R. Ganzerla, Appl. Catal. A 201 (1999) 263.
- [3] U. Freese, F. Heinrich, F. Roessner, Catal. Today 49 (1999) 237.
- [4] H.W. Kouwenhoven, R. Fang, G. Harvey, R. Prins, Appl. Catal. A 130 (1995) 67.
- [5] K. Gaare, D. Akporiaye, J. Mol. Catal. A 109 (1996) 177.
- [6] A.K. Pandey, A.P. Singh, Catal. Lett. 44 (1997) 129.
- [7] B. Chiche, A. Finiels, C. Gauthier, P. Geneste, J. Mol. Catal. 42 (1987) 229.
- [8] K. Okumura, K. Nishigaki, M. Niwa, Micropor. Mesopor. Mater. 44 (2001) 509.
- [9] J.A. Melero, R. van Grieken, G. Morales, V. Nuno, Catal. Commun. 5 (2004) 131.
- [10] J.J. Chiu, D.J. Pine, S.T. Bishop, B.F. Chmelka, J. Catal. 221 (2004) 400.
- [11] M. Alvaro, A. Corma, D. Das, V. Fornés, H. García, J. Catal. 231 (2005) 48.
- [12] V.R. Choudhary, S.K. Jana, J. Catal. 201 (2001) 225.
- [13] N.B. Shrigadi, A.B. Shinde, S.D. Samant, Appl. Catal. A 252 (2003) 23.
- [14] K. Mantri, K. Komura, Y. Kubota, Y. Sugi, J. Mol. Catal. A 236 (2005) 168.
- [15] V.R. Choudhary, R. Jha, V.S. Narkhede, J. Mol. Catal. A 239 (2005) 76.
- [16] O.S. Ahmed, D.K. Dutta, J. Mol. Catal. A 229 (2005) 227.
- [17] T. Nishimura, S. Ohtaka, K. Hashimoto, T. Yamauchi, T. Hasegawa, K. Imanaka, J. Tateiwa, H. Takeuchi, S. Uemura, Bull. Chem. Soc. Jpn. 77 (2004) 1765.
- [18] K. Okumura, K. Yamashita, M. Hirano, M. Niwa, Chem. Lett. 34 (2005) 716.
- [19] P. Metivier, in: R.A. Sheldon, H. van Bekkum (Eds.), Fine Chemicals Through Heterogeneous Catalysis, Wiley/VCH, Weinheim, 2001, p. 161.
- [20] E.G. Derouane, G. Crehan, C.J. Dillon, D. Bethell, H. He, S.B.A. Hamid, J. Catal. 194 (2000) 410.

- [21] F. Jayat, M.J.S. Picot, M. Guisnet, *Catal. Lett.* 41 (1996) 181.
- [22] A. Vogt, H.W. Kouwenhoven, R. Prins, *Appl. Catal. A* 123 (1995) 37.
- [23] G. Winé, J. Matta, J.-P. Tessonnier, C. Pham-Huu, M.-J. Ledoux, *Chem. Commun.* 530 (2003).
- [24] A.M.F. Bidart, A.P.S. Borges, L. Nogueira, E.R. Lachter, C.J.A. Mota, *Catal. Lett.* 75 (2001) 155.
- [25] C. Hardacre, S. Katdare, D. Milroy, P. Nancarrow, D.W. Rooney, J.M. Thompson, *J. Catal.* 227 (2004) 44.
- [26] E.G. Derouane, I. Schmidt, H. Lachas, C.J.H. Christensen, *Catal. Lett.* 95 (2004) 13.
- [27] T. Okuhara, N. Mizuno, M. Misono, *Adv. Catal.* 41 (1996) 113.
- [28] Y. Izumi, K. Urabe, M. Onaka, *Zeolite, Clay and Heteropolyacids in Organic Reactions*, Kodansha/VCH, Tokyo/Weinheim, 1992.
- [29] I.V. Kozhevnikov, *Chem. Rev.* 98 (1998) 171.
- [30] T. Okuhara, N. Mizuno, M. Misono, *Appl. Catal. A* 222 (2001) 63.
- [31] T. Okuhara, *Catal. Today* 73 (2002) 167.
- [32] J. Kaur, K. Griffin, B. Harrison, I.V. Kozhevnikov, *J. Catal.* 208 (2002) 448.
- [33] C. Castro, J. Primo, A. Corma, *J. Mol. Catal. A* 134 (1998) 215.
- [34] J. Kaur, I.V. Kozhevnikov, *Chem. Commun.* (2002) 2508.
- [35] I.V. Kozhevnikov, *Appl. Catal. A* 256 (2003) 3.
- [36] T. Tagawa, J. Amemiya, S. Goto, *Appl. Catal. A* 257 (2004) 19.
- [37] J.R. Johnson, *Org. React.* 1 (1942) 248.
- [38] L.A. Mitscher, *European Patent* 63945 (1982).
- [39] J. Mao, T. Nakajyo, T. Okuhara, *Chem. Lett.* 31 (2002) 1104.
- [40] K.Y. Jung, M. Koreeda, *J. Org. Chem.* 54 (1989) 5667.
- [41] J. Mao, Y. Kamiya, T. Okuhara, *J. Mol. Catal. A* 255 (2003) 337.
- [42] T. Okuhara, H. Watanabe, T. Nishimura, K. Inumaru, M. Misono, *Chem. Mater.* 12 (2000) 2230.
- [43] L. Li, Y. Yoshinaga, T. Okuhara, *Phys. Chem. Chem. Phys.* 1 (1999) 4913.
- [44] G.I. Kapustin, T.R. Brueva, A.L. Klyachko, M.N. Timofeeva, S.M. Kulikov, I.V. Kozhevnikov, *Kinet. Catal.* 31 (1990) 896.
- [45] V.M. Mastihkin, S.M. Kulikov, A.V. Nosov, I.V. Kozhevnikov, I.L. Mudrakovsky III, M.V. Timofeeva, *J. Mol. Catal.* 60 (1990) 65.
- [46] F. Lefebvre, *J. Chem. Soc., Chem. Commun.* (1992) 756.
- [47] A. Miyaji, T. Echizen, K. Nagata, Y. Yoshinaga, T. Okuhara, *J. Mol. Catal. A* 201 (2003) 145.
- [48] A. Miyaji, R. Ohnishi, T. Okuhara, *Appl. Catal. A* 262 (2004) 143.